Spreading of a solid-on-solid drop

J. De Coninck
Faculté des Sciences, Université de Mons-Hainaut, 20, Place du Parc, 7000 Mons, Belgium

F. Dunlop
Centre de Physique Théorique, Ecole Polytechnique, 91128 Palaiseau CEDEX, France

F. Menu
Faculté des Sciences, Université de Mons-Hainaut, 20, Place du Parc, 7000 Mons, Belgium
(Received 14 May 1992)

We study the spreading of the foot of a two-dimensional drop via Monte Carlo simulations without conservation law. The profile, or height of the spreading phase as a function of the distance from the initial drop, is described by a solid-on-solid model. For positive spreading coefficients, we find a precursor film extending linearly with time, and thickening as $t^{1/4}$ due to entropic repulsion. For a vanishing spreading coefficient, i.e., at the wetting transition, the foot of the profile is found to scale as $t^{1/2}$ parallel and perpendicular to the substrate, with no precursor asymptote. For partial wetting, relaxation is checked against exact results including finite-size effects.

PACS number(s): 68.10.Gw, 05.50.+q

Spreading of liquids on solids has been a very active field of research rather recently. Beautiful experiments have been performed [1–5], showing in some cases a precursor film of molecular thickness and length proportional to $\sqrt{t}$. Several attempts have been made to understand this behavior. Up to how, however, the only model that seems to capture the experimental data was based on hydrodynamics at a molecular level [6].

Relaxation to equilibrium of model systems can be described in a reliable fashion by stochastic evolutions, like Langevin or Monte Carlo dynamics, which work at length scales that are intermediate between molecular and macroscopic. It is therefore natural to ask for the prediction of stochastic dynamics in the case of spreading. This is the motivation of the present paper, where we consider a stochastic approach of spreading, with particular attention to entropic repulsion effects. A suitable model for this study is the columnar solid-on-solid (SOS) model, where the variables describe the height of the interface above the substrate. A self-avoiding-walk model has been studied recently [7] in the same spirit, with valuable results, but the SOS model is easier to handle, both exactly and numerically, which allows us to give more precise results. Previous work [8–10] used "parallel" SOS models, where the variables describe layers parallel to the substrate. This had the advantage of allowing Langevin dynamics, but could not take into account the entropic repulsion associated with an inpenetrable substrate.

We consider a macroscopic droplet on a wall in a system of two phases A and B, which are at equilibrium in the bulk. The main object of our study is the time behavior of the foot of the drop, which we take initially as a wedge of length l_0 and height h_0, as reproduced in Fig. 1. This length l_0 has to be taken large (going to infinity in the thermodynamic limit), but much smaller than the size of the macroscopic drop; we then study the time evolution up to t less than l_0^2. The interface at time t is described by heights $h_0, h_1, \ldots, h_{l_t} \in \mathbb{N}$, with $h_i \geq 1$ for $i-0, \ldots, l_t$ and $h_j = 0$ for $j > l_t$.

The model is the restricted-solid-on-solid (RSOS) model with $h_{i+1} - h_i \in \{-1, 0, 1\}$ and the Hamiltonian:

$$H(h_0, \ldots, h_l) = \sum_{i=0}^{l-1} J[|h_{i+1} - h_i| + 1] + l(\sigma_{BW} - \sigma_{AW}) , \tag{1}$$

where $\sigma_{BW} - \sigma_{AW}$ represents the difference of wall free energies, and l is a random variable that measures the spreading of the drop. These wall free energies incorporate a contact potential at the wall and can be computed exactly in some model cases [11]. The coefficient J is the energy per unit length of the A-B interface. The boundary condition is fixed by $h_0 = \text{const}$. The corresponding

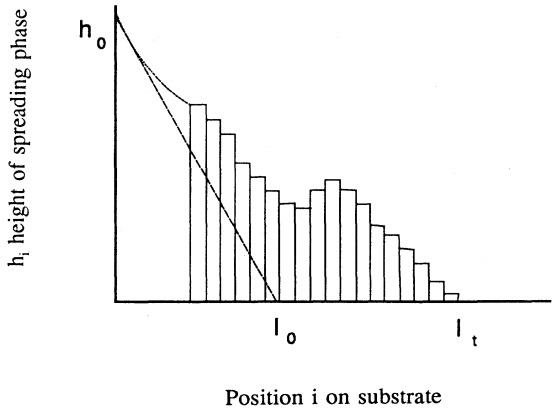

FIG. 1. Wedge of height h_0 and length l_0 and example of SOS profile of length l_t.

equilibrium partition function is

$$Z(h_0)=\sum_{l=0}^{+\infty}\sum_{\{h_1,\ldots,h_l\}} e^{-\beta H(h_0,\ldots,h_l)} . \quad (2)$$

A significant feature of the model is that the equilibrium mean value of l and all its subsequent moments can be exactly computed for any choice of h_0. Finite-size effects can thus be exactly computed, which is important for appropriate analysis of relaxation. The computation goes as follows. For $h_0=1$, we find, in the spirit of Ref. [12], that $Z(1)$ satisfies

$$Z(1)=\frac{ac}{1-c}+\frac{acZ^2(1)}{1-c} , \quad (3)$$

where

$$a=e^{-J/kT} ,$$
$$c=e^{-(J+\sigma_{BW}-\sigma_{AW})/kT} .$$

The first term of (3) is the contribution of interfaces with $h_i \le 1$ for all i. The mean value and variance of l are then obtained by

$$\langle l\rangle_1=\frac{\partial \ln Z(1)}{\partial \ln c}=\frac{1}{[(1-c)^2-4a^2c^2]^{1/2}} , \quad (4)$$

$$\langle l^2\rangle_1-\langle l\rangle_1^2=\frac{\partial^2 \ln Z(1)}{\partial(\ln c)^2} . \quad (5)$$

In general, h_0 will typically be large at the molecular scale and small at the scale of the drop. We have exactly

$$Z(h_0)=[Z(1)]^{h_0} , \quad (6)$$

and thus

$$\langle l\rangle_{h_0}=h_0\langle l\rangle_1=\frac{h_0}{[(1-c)^2-4a^2c^2]^{1/2}} , \quad (7)$$

$$\langle l^2\rangle h_0-\langle l\rangle_{h_0}^2=h_0\{\langle l^2\rangle_1-\langle l\rangle_1^2\} . \quad (8)$$

The contact angle θ of the drop with the substrate can be defined by

$$\tan\theta=\lim_{h_0\to\infty}\frac{h_0}{\langle l\rangle_{h_0}} .$$

In the present model, the above ratio happens to be independent of h_0, as is obvious from Eq. (7). The resulting contact angle can be checked to verify Young's equation generalized to anisotropic media [13]

$$\sigma_{AB}(\theta)\cos\theta-\sigma'_{AB}(\theta)\sin\theta=\sigma_{AW}-\sigma_{BW} ,$$

where $\sigma_{AB}(\theta)$ is the interfacial tension of an A-B interface at angle θ, defined with the Hamiltonian (1) but in the absence of a wall, and $\sigma'_{AB}(\theta)$ is the derivative of $\sigma_{AB}(\theta)$ with respect to θ. The term $\sigma'_{AB}(\theta)\sin\theta$ is, of course, identically zero for isotropic fluids, but cannot be neglected in the interpretation of numerical work on lattice models.

The above formulas give finite results only in the partial-wetting regime, which is conveniently characterized by a negative spreading coefficient,

$$s=\sigma_{AW}-\sigma_{BW}-\sigma_{AB}(\theta=0)<0 , \quad (9)$$

where

$$\sigma_{AB}(\theta=0)=J-kT\ln(1+2e^{-J/kT}) . \quad (10)$$

As $s\to 0$, we get

$$\langle l\rangle_{h_0}\simeq\frac{c}{1-c}\frac{1-c+4a^2c}{\sqrt{1-c+2ac}}\frac{h_0}{\sqrt{-s}}=O\left[\frac{h_0}{\sqrt{-s}}\right] , \quad (11)$$

$$\langle l^2\rangle_{h_0}-\langle l\rangle_{h_0}^2\simeq\frac{c^2}{1-c}\frac{(1-c+4a^2c)^2}{(1-c+2ac)^{3/2}}\frac{h_0}{(-s)^{3/2}}$$
$$=O\left[\frac{h_0}{(-s)^{3/2}}\right] . \quad (12)$$

To study the relaxation to equilibrium, we have considered the Monte Carlo (MC) dynamics associated with the model. The corresponding stochastic process is ergodic and satisfies detailed balance. We have chosen the RSOS ($h_{i+1}-h_i\in\{-1,0,1\}$) rather than the SOS model in order to satisfy conveniently this detailed-balance condition. We recall that these conditions imply convergence to equilibrium. We have indeed checked that the time averages of l_t and l_t^2 converge to the equilibrium values $\langle l\rangle_{h_0}$ and $\langle l^2\rangle_{h_0}$ computed above. The relaxation time τ is of order l^2, which thus requires l^3 MC steps. As the wetting transition is approached ($s\to 0$), the corresponding slowing down can be estimated by

$$\langle l^3\rangle\simeq\langle l\rangle^3(-s)^{-1}\simeq(-s)^{-5/2} .$$

We also obtain mean profiles, which cannot be computed exactly, as represented in Fig. 2, where the effect of entropic repulsion is clear. The curvature of the mean profile near the substrate can indeed only come from entropic repulsion, because we only have a contact interaction with the wall. In more complicated models, entropic repulsion is buried with other interactions.

Let us now consider the complete wetting regime with $s>0$ or $s=0$, for which the drop will spread out indefinitely. We are in this case interested in the shape of the spreading edge and precursor films ($s>0$). We use

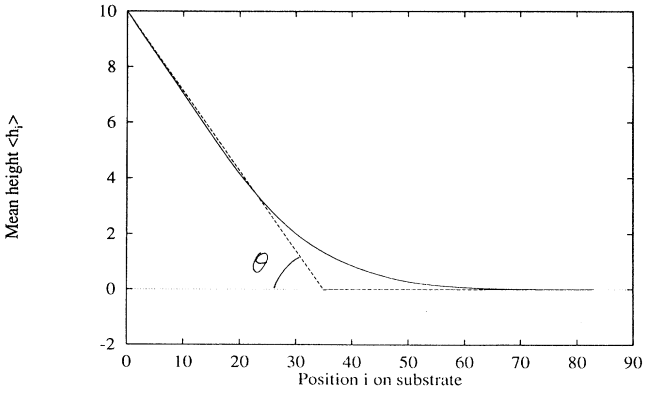

FIG. 2. Equilibrium profile for partial wetting showing the entropic repulsion effect near the wall ($J/kT=1$, $s=-0.1$). θ is the exact equilibrium contact angle.

the same algorithm as before.

For $s>0$, analogous to "dry spreading," we get that l_t goes linearly with time, which is measured as the number of MC steps per site. Let us stress that the dynamics considered here does not locally conserve the respective volume of the two phases, and therefore a diffusive behavior is not to be expected. The speed as a function of the spreading parameter s is represented in Fig. 3. We have obtained this speed in two ways, with a good agreement between the two results: (a) $S_{\text{speed}}=\lim_{t\to\infty}(l_t-l_0)/t$; (b) given that $h_{l_t+1}=0$ and $h_{l_t}=1$, the asymptotic speed is given analytically in terms of $\langle h_{l_t-1}\rangle$ by

$$S_{\text{speed}}=1-\frac{(1+2e^{-J/kT})(3-\langle h_{l_t-1}\rangle)}{1+2e^{-J/kT}+e^{s}} .$$

The maximum speed is one, because each update of the profile can at most increase l_t by 1.

The thickening of the precursor film can be described as follows: the height $h_i(t)$ at point i is proportional to the one-fourth-power of the time elapsed since the precursor film reached at this point. This $t^{1/4}$ law yields a profile $h_i\sim(l_t-i)^{1/4}$. Figure 4 represents a log-log plot of this profile.

This behavior can be understood by comparison to the fluctuation of an interface in the absence of a wall: if we would remove the restriction $h_i\geq 0$, the fluctuations would be $\simeq t^{1/4}$, as shown explicitly in Langevin dynamics [14,8]. The wall condition $h_i\geq 0$ causes entropic repulsion of the same amplitude as the fluctuations that the wall prevents.

The thickening of the precursor film is clearly related to the growth of wetting layers, starting from a completely dry situation. The $t^{1/4}$ law for this case has been predicted by scaling arguments [15] and obtained from Monte Carlo simulations [16–19].

We now describe the foot of the profile, which makes a smooth function between the drop and the precursor film. We find that this foot scales as $t^{1/2}$ in both directions, i.e.,

$$\frac{h(l_0+xt^{1/2})-h_0(l_0+xt^{1/2})}{t^{1/2}}\to\phi(x) \quad \text{as } t\to\infty ,$$

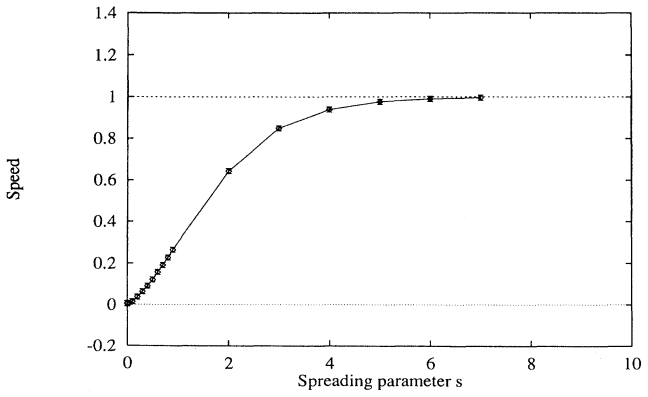

FIG. 3. Speed as a function of the spreading parameter s.

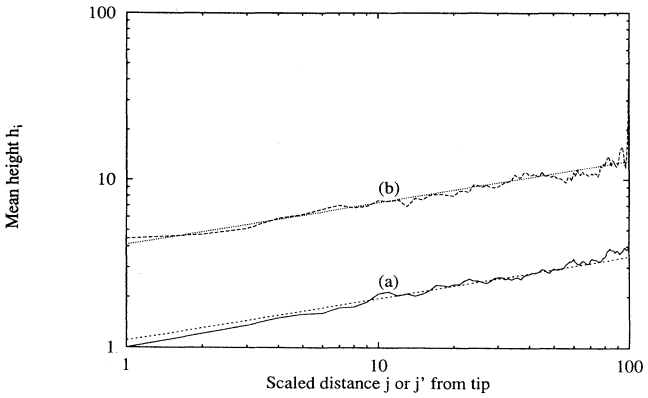

FIG. 4. Log-log plot of the height h_i of the precursor film (a) vs the distance $j=l_t-i$ between the tip l_t and the point i, with $j=1,\ldots,100$; (b) vs a scaled distance $j'=100\ (l_t-i)/(l_t-l_0)$ with $j'=1,\ldots,100$. The dotted line represents straight lines of slope $\frac{1}{4}$ ($J/kT=1$, $s=1.0$, averages are taken with l_t varying from 6000 to 48 000).

which is in agreement with the analogous result for the parallel SOS model with Langevin dynamics [8]. The approximation to $\phi(x)$ obtained as time averages from the MC simulations is shown in Fig. 5(a).

We expect $\phi(x)\equiv 0$ for $x>\text{const}\simeq 1.7$, but the finite time averages approximate $\phi(x)$ with an error decaying only as $t^{-1/4}$, which is implied by the junction with the precursor film.

The scale-invariant shape of the foot of the drop, associated with $\phi(x)$, indicates that the scaling arguments developed in Ref. [8] in connection with Langevin dynamics should apply also to the present model. The dynamic shape obtained here (no asymptote) is, however, physically more satisfactory than that obtained for the parallel SOS model [$\phi(x)\to 0$ as $x\to\infty$]. Analogous differences appear in the Winterbottom droplet equilibrium shapes for these two SOS models.

We now turn to $s=0$, which may be considered as moist spreading. This case can indeed by obtained from the previous case, $s>0$, by adding into the initial condition a monolayer covering the wall. Figure 6 shows

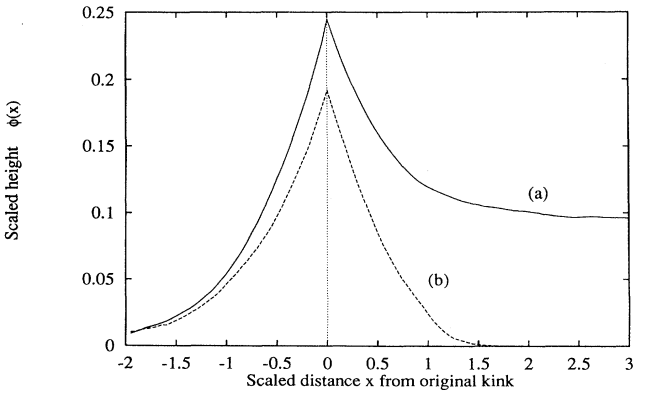

FIG. 5. Scaling profiles $\phi(x)$ obtained from time averages from MC simulations with l_t varying from 4000 to 6000 for $s=0.7$ (a) and with 4×10^6 MC steps/site for $s=0$ (b).

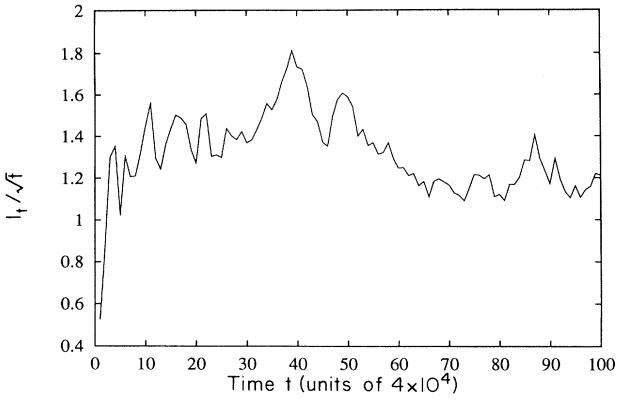

FIG. 6. $l_t/\sqrt{t}$ for $s=0$ ($t_{\max}=4\times10^6$ MC steps/site, $J/kT=1$)

$l_t/\sqrt{t}$ as a function of t, where t is again the number of MC steps per site. The curve indicates that a logarithmic correction is very unlikely.

The foot of the profile scales as in the case where $s>0$. The approximation to the scaling function obtained from the simulations with $s=0$ is reproduced in Fig. 5(b). The scaling functions for $s>0$ and for $s=0$ appear to be very similar; the difference can be accounted for by a systematic overestimate in the case $s>0$ due to the junction with the precursor film of height $\sim t^{1/4}$. This error decays as $t^{-1/4}$, and longer simulations should bring the two curves together. Another significant feature is the absence of an asymptote, which might have been taken as a precursor film. Indeed, our simulations have given

$$h_{l_0+1.7\sqrt{t}}(t)\equiv 0 \quad \text{for any } t\leq 4.10^6 \text{ MC steps/site} .$$

This result confirms the absence of logarithmic corrections to the $\sqrt{t}$ behavior of the spreading length l_t in the case of moist spreading $s=0$.

The authors thank the CNRS, the FNRS, and CGRI for their financial support, which made this collaboration possible. This text also presents research results of the Belgian Programme on Interuniversity Poles of Attraction initiated by the Belgian State, Prime Minister's Office, Science Policy Programming.

[1] F. Heslot, A. M. Cazabat, and P. Levinson, Phys. Rev. Lett. **62**, 1286 (1989).
[2] F. Heslot, N. Fraysse, and A. M. Cazabat, Nature **338**, 640 (1989).
[3] F. Heslot, N. Fraysse, A. M. Cazabat, P. Levinson, and P. Carles, in *Wetting Phenomena,* edited by J. De Coninck and F. Dunlop (Springer-Verlag, Berlin, 1989).
[4] L. Leger, M. Erman, A. M. Guinet-Picard, D. Ausserre, and C. Strazielle, Phys. Rev. Lett. **60**, 2390 (1988).
[5] D. Beaglehole, J. Phys. Chem. **93**, 893 (1989).
[6] P. G. de Gennes and A. M. Cazabat, C. R. Acad. Sci. **310**, 1601 (1990).
[7] J. Cook and D. E. Wolf, J. Phys. A **24**, L351 (1991).
[8] D. B. Abraham, P. Collet, J. De Coninck, and F. Dunlop, Phys. Rev. Lett. **65**, 195 (1990); J. Stat. Phys. **61**, 509 (1990).
[9] D. B. Abraham, J. Heiniö, and K. Kaski, J. Phys. A **24**, L309 (1991).
[10] B. Chopard, J. Phys. A **24**, L345 (1991).
[11] J. De Coninck and F. Dunlop, Europhys. Lett. **4**, 1291 (1987).
[12] M. Fisher, J. Stat. Phys. **34**, 667 (1984).
[13] J. De Coninck and F. Dunlop, J. Stat. Phys. **47**, 827 (1987).
[14] D. B. Abraham and P. J. Upton, Phys. Rev. B **39**, 736 (1989).
[15] R. Lipowski, J. Phys. A **18**, L585 (1985).
[16] K. Binder and D. P. Landau, *Advances in Chemical Physics,* edited by K. P. Lawley (Wiley, New York, 1989), Vol. 76, p. 91.
[17] K. Binder, in *Kinetics of Ordering and Growth at Surfaces,* edited by M. G. Lagally (Plenum, New York, 1990), p. 31.
[18] E. V. Albano, K. Binder, D. W. Heermann, and W. Paul, Surf. Sci. **223**, 151 (1989).
[19] E. V. Albano, K. Binder, D. W. Heermann, and W. Paul, Physica A **183**, 130 (1992).